Eur. J. Solid State Inorg. Chem.
t. 28, 1991, p. 335-346

Chemistry of the rare earth elements in the solar nebula

B. FEGLEY

Lunar and Planetary Institute, 3303 NASA Road 1, Houston, TX 77058, U.S.A.
and Abteilung Kosmochemie*, Max Planck Institut für Chemie, Saarstrasse 23,
6500 Mainz, Germany

T. R. IRELAND

Research School of Earth Sciences, The Australian National University,
Canberra ACT 2601, Australia

ABSTRACT.–The rare earth elements (La to Nd and Sm to Lu) are trace elements found at sub-ppm to ppm levels in chondritic meteorites. Although their abundances (normalized to mean chondrites) are generally smooth at the ±20% level, high precision analyses reveal numerous anomalies. Some anomalies (Eu) are consistent with planetary processes while others (Ce and Yb) are probably signatures of condensation processes in the solar nebula. Phosphate minerals in equilibrated ordinary chondrites, Ca, Al-rich inclusions (CAIs), predominantly found in the oxidized carbonaceous chondrites, and oldhamite (CaS), found in the reduced enstatite chondrites, are highly enriched in the REE relative to their concentration in the bulk meteorites. The REE enrichments in phosphates are consistent with redistribution during metamorphism. The REE abundance patterns observed in CAIs fall into two broad categories: (1) generally smooth, unfractionated patterns which may have Eu and Yb anomalies, and (2) highly irregular fractionated patterns which have a complex structure. The unfractionated patterns can result either from vaporization or condensation processes in the solar nebula. However, the highly irregular (Group II) patterns must result from a fractional condensation process because both the most refractory and the most volatile REE are depleted in them. The limited data available on REE abundance patterns in CaS show only relatively unfractionated patterns and no analogs to the highly irregular Group II patterns frequently seen in CAIs. We review relevant analytical data for REE in CAIs and oldhamite and then discuss several implications of the observed REE patterns for chemical and physical conditions during the formation of these meteorite components. In particular, we emphasize the apparent discrepancy between the high temperatures required for formation of the Group II REE patterns and the isotopic anomalies in Ca and Ti in these CAIs. The REE, Ca, and Ti have similar volatilities and Ca and Ti would be vaporized and isotopically homogenized at the temperatures needed to explain the Group II patterns. This problem is unresolved and is an important question in cosmochemistry.

* Correspondence address

REE ABUNDANCES IN CHONDRITIC METEORITES

The first REE analyses of meteorites were done in 1935 by Noddack [1] who used an emission spectrographic technique to measure the REE in a mixture of chondritic (90%) and achondritic (10%) meteorites. However, data of satisfactory quality for determining the elemental abundances of the REE and for testing models of nucleosynthesis of the elements did not appear until the early 1960's when neutron activation analysis was first used for REE determinations in meteorite samples [2]. REE analyses in bulk chondrites have also been done by isotope dilution mass spectroscopy. Anders and Grevesse [3] review bulk chondrite analyses used to determine the solar (i.e., C1 chondrite) abundances of the REE. Their recommended values for the REE solar abundances are reproduced in Table 1. Unless stated otherwise, all REE abundance patterns (bulk meteorite, CAIs, etc.) discussed in this paper are normalized to C1 chondrite abundances in order to remove the sawtooth pattern resulting from the nucleosynthesis abundance trends for even/odd mass number nuclei [4].

TABLE I. Abundances of the REE

Element	REE Atoms per 10^6 Si Atoms	ppm by mass
57. La	0.446	0.235
58. Ce	1.136	0.603
59. Pr	0.167	0.089
60. Nd	0.828	0.452
62. Sm	0.258	0.147
63. Eu	0.097	0.056
64. Gd	0.330	0.197
65. Tb	0.060	0.036
66. Dy	0.394	0.243
67. Ho	0.089	0.056
68. Er	0.251	0.159
69. Tm	0.038	0.024
70. Yb	0.248	0.162
71. Lu	0.037	0.024

Analyses of bulk chondrites also provide clues to the chemical processes that chondrites have undergone. With the possible exception of the EL chondrites, all chondrite classes have the same relatively unfractionated REE patterns, although at different absolute abundance levels [5]. As discussed by Larimer and Wasson [6], these differences probably result from two processes: (1) dilution of a refractory lithophile component by different amounts of less refractory material and (2) nebular fractionation of refractory lithophiles as a group. Removing the dilution effect by normalization to Si gives the well known sequence CV > CM ~ CO > H ~ L > LL > EH > EL for the amounts of refractory lithophiles in the different chondrite classes. The mechanism for this fractionation is unknown but may involve the accretion of variable amounts of CAI-like material by the different chondrite groups [6].

Evensen *et al* [7] give a detailed discussion of neutron activation and isotope dilution analyses of bulk chondrites. They find that relative to mean chondritic abundances, the REE patterns in chondrites are generally smooth at the ±20% level, but display numerous anomalies, particularly in Eu and Ce. Evensen *et al* persuasively argue that many of these anomalies such as Eu depletions/enrichments are consistent with geochemical processes on planetary bodies but emphasize that other anomalies (e.g., in Ce and Yb) are probably

signatures of fractional condensation processes in the solar nebula. Likewise, Fegley and Kornacki [8] contended that the abundances of the REE in the bulk Allende meteorite are not smooth but instead show the signature of the fractionated Group II REE pattern.

Finally, the REE distribution in ordinary chondrites has been studied by using selective dissolution or heavy liquid separation to isolate different mineral phases which are then analyzed for the REE (e.g., [9]). The results show that a large fraction of the REE (except Eu) in equilibrated ordinary chondrites are in the phosphate minerals merrillite $Ca_3(PO_4)_2$ and apatite $Ca_5(PO_4)_3(Cl,OH,F)$. In contrast, Eu is concentrated in feldspars (presumably as Eu^{2+}). More recently, ion microprobe analyses of phosphates from equilibrated ordinary chondrites (e.g., [10]) have confirmed these results. Several of the chondrites analyzed by ion microprobe techniques (e.g., Guareña, Bruderheim, Forest City, Richardton) have anomalous bulk REE patterns [7]; however, no unequivocal abundance anomalies were reported in the ion microprobe analyses. In some cases the ion probe analyses do not include the putatively anomalous REE, while in other cases the anomaly involves Eu and would be difficult to distinguish solely from the phosphate analyses which generally show large Eu depletions. Unfortunately, neither the most anomalous chondrites (Khohar, Modoc, Vavilovka), nor unequilibrated ordinary chondrites have been studied by ion microprobe.

REE ANALYSES IN Ca,Al-RICH INCLUSIONS

analyses of CAIs in the Allende meteorite

Briefly, Ca,Al-rich inclusions (CAIs) are refractory objects that are predominantly found in the carbonaceous chondrites, although they are also found at lower volumetric abundance in the ordinary and enstatite chondrites [11-12]. Their chemistry and mineralogy has recently been reviewed by MacPherson *et al* [13]. These objects first attracted widespread attention after they were reported in the Allende carbonaceous chondrite [14]. Representative CAIs from Allende are illustrated by MacPherson *et al* [13] and representative CAIs from the Murchison carbonaceous chondrite are illustrated in Figure 1.

The mineralogy of Allende CAIs is dominated by Ca,Al,Ti-bearing minerals such as melilite, a solid solution of gehlenite ($Ca_2Al_2SiO_7$) and åkermanite ($Ca_2MgSi_2O_7$), pyroxene, mainly diopside ($CaMgSi_2O_6$) with significant substitution of Al and Ti, and spinel ($MgAl_2O_4$). Minor amounts of hibonite ($CaAl_{12}O_{19}$) and perovskite ($CaTiO_3$) are also commonly present. Marvin *et al* [15] first described several Allende CAIs and noted that their chemistry and mineralogy resembles that predicted for high temperature condensates from a totally vaporized solar composition gas [16,17]. This observation is correct to first approximation; however, subsequent studies of CAI chemistry and mineralogy [18-20] show that observed mineral assemblages in many CAIs disagree in detail with the mineral assemblages predicted for condensation in the solar nebula [21].

At about the same time as the initial description of Allende CAIs by Marvin *et al*, Gast *et al* [22] published the first REE analysis for a CAI. Later CAI analyses by Grossman [23] and Wänke *et al* [24] showed that refractory elements (Al, Ca, Ti, Sc, Y, Zr, Nb, Hf, Ta, W, U, Re, Os, Ir, Ru, Pt, and the REE), which otherwise behave differently during geochemical processes such as magmatic differentiation, were rather uniformly enriched by ~20 times relative to their C1 chondrite abundances. This enrichment was attributed to condensation of the most refractory 5% of chondritic matter from the solar nebula.

However, as first shown by Tanaka and Masuda [25], in some cases the REE abundance

patterns in CAIs are highly irregular and display large fractionations. This type of pattern is characterized by relatively high enrichments of the light REE (LREE) and rapidly diminishing abundances of the HREE. Superimposed on this overall pattern are positive anomalies in Tm and Yb and a negative anomaly in Eu. Martin and Mason [26] subsequently found more examples of this highly irregular REE abundance pattern, which they termed Group II patterns. Table 2 shows that ~34% of all CAIs analyzed have Group II patterns.

Mason and colleagues [26-28] further subdivided CAIs with unfractionated REE patterns into four groups on the basis of Eu and Yb anomalies. Group I CAIs have positive Eu anomalies, Group V CAIs have no Eu or Yb anomalies, Group III CAIs have negative Eu and Yb anomalies, and Group VI CAIs have positive Eu and Yb anomalies which are roughly complementary to the negative Eu and Yb anomalies in Group III CAIs. Martin and Mason [27] also recognized another unfractionated REE group, called Group IV, but this is made up of olivine-rich objects, which are not CAIs. Examples of all six REE patterns and REE abundances in bulk Allende are shown in Figure 2 [25-30]. However, the spark source analyses for the Group IV and VI CAIs do not include Lu [27-28].

The relative abundance of the different patterns is listed in Table 2, which is compiled from a large number of literature references [31]. However, the statistics in Table 2 are biased by Allende CAIs. Larger, coarse-grained, Allende CAIs (mm to cm in size), which are more easily seen and extracted from specimens, have been analyzed more frequently than smaller, fine-grained, Allende CAIs which are less prominent and more difficult to extract. The larger CAIs frequently have Group I and V REE patterns while the smaller CAIs frequently have Group II and III REE patterns. However, as indicated by a comprehensive petrographic survey of all objects with diameters $\geq 200\mu m$ in polished thin sections from Allende, the smaller, fine-grained CAIs with Group II and III REE patterns may in fact be more abundant [32-33]. The overall abundance of Group II CAIs in Allende is also suggested by the fractionated bulk Allende REE pattern as illustrated in Figure 2.

analyses of CAIs in the Murchison meteorite

In contrast to CAIs from Allende, those from Murchison are much smaller, typically less than 200 μm, and are composed predominantly of hibonite, spinel, perovskite, and occasionally corundum (Al_2O_3). As reviewed by Boynton [34], the REE analysis of a Murchison CAI first revealed the complementary pattern to the Allende Group II pattern, i.e., enriched in the ultrarefractory elements. Ekambaram *et al* [35] studied ten inclusions from Murchison and found that they also had highly fractionated REE patterns. They subdivided the patterns into four categories: (1) Group II patterns similar to those in Allende (with modified abundances of Eu and Yb), (2) Group III patterns similar to those in Allende but with a rolloff in the heavy REE, (3) patterns with large Yb anomalies unaccompanied by Eu anomalies, and (4) the ultrarefractory enriched pattern.

Subsequent work on Murchison CAIs is dominated by ion microprobe measurements where hibonite and perovskite have been found to be the major repositories of the REE. Some 86 hibonite-bearing inclusions have been analyzed for their trace element abundances ([36] and references therein). These are mainly from Murchison (81 CAIs), but inclusions from other meteorites have also been studied. The classification of these CAIs according to their REE patterns (see Table 2) reveals that the vast majority of Murchison CAIs have Group II and Group III patterns in contrast to the high proportion of Group I,V CAIs

in Allende. Canonical Group II patterns are occasionally found, but more commonly the patterns are characterized by variable abundances of the LREE and variable abundances of Eu and Yb. This pattern is exemplified in three perovskites analyzed by Ireland *et al* [36] and the mean pattern of these three is shown in Figure 2.

The LREE abundances in this mean perovskite Group II pattern are complementary to those in the mean hibonite ultrarefractory pattern observed in four Murchison CAIs (Fig.2). This suggests that the pattern is the result of fractionation of the LREE in a similar fashion to the HREE. In this case, the removal of the ultrarefractory component responsible for the Group II pattern took place at a lower temperature when a significant fraction of the LREE had condensed from the gas. The enrichment in the ultrarefractory elements is shown by the elevated abundance of Gd relative to the LREE and Eu; however, the enrichment tails off with Lu only as abundant as the LREE. This contrasts with the ultrarefractory patterns found in other CAIs (e.g., in Ornans) where Lu is the most abundant REE. The roll-off in HREE abundances may be due to some form of igneous fractionation; however, the phase which might take up the missing HREE component is not present in these CAIs.

Depletions of the HREE according to ionic radius are also apparent in the Group III CAIs found in Murchison. Again however, there is no phase present which might take up the HREE. The Murchison Group III pattern also differs from the Allende counterpart in that the Yb depletions are generally larger than the Eu depletions whereas they are subequal in Allende. The reason for this is not clear since Eu is predicted to be more volatile than Yb and so depletions caused by vaporization or incomplete condensation should manifest themselves in Eu to a greater extent than in Yb.

Isotopic analyses of Mg, Ca, and Ti made on a large number of Murchison CAIs reveal a number of remarkable correlations linking the isotopic systematics with the chemistry [37]. The Ca and Ti isotopic compositions of Murchison CAIs often show large anomalies, both excesses and deficits, in the heaviest isotopes ^{48}Ca and ^{50}Ti. These anomalies represent incomplete mixing of nucleosynthetic components which comprise the solar system abundances of these elements. On the other hand, Mg isotopic compositions often show excesses from the decay of radiogenic ^{26}Al ($t_{1/2} \sim 0.7$ Ma). The canonical abundance of ^{26}Al in the early solar system is $(^{26}Al/^{27}Al)_0 \sim 5 \times 10^{-5}$, which is the maximum abundance found in a large number of CAIs. No inclusion has been found in Murchison which has both large Ti isotopic anomalies and excess ^{26}Mg at a level of 50 ppm $\times ^{27}$Al. However, all Group II CAIs have ^{26}Al abundances at this level with the exception of those that have large Ti isotopic anomalies. These characteristics of mutual exclusivity are particularly evident in two spinel hibonite spherules, 7-734 and 7-170, which are shown in Figure 1e and f. The morphological similarity of these two inclusions is also matched by their similar REE patterns (both of which are Group II patterns). However, the isotopic systematics are quite different with 7-734 possessing normal Ti isotopic abundances and $(^{26}Al/^{27}Al)_0 \sim 5 \times 10^{-5}$ while 7-170 has a 5% deficit in ^{50}Ti and very little excess ^{26}Mg.

Another interesting point is that $\sim$ 30% (24/81) of all Murchison CAIs analyzed [31] have Ce anomalies. These are split almost evenly between depletions (10) and enrichments (14). This is dramatically different from Allende where only two CAIs with Ce depletions have been found, giving a frequency of $\sim$2% [31]. A recent re-analysis [38] of one of these two CAIs (C1) does not show a Ce depletion (the normalized La/Ce ratio is $\sim$1); the discrepancy with the previous work (normalized La/Ce $\sim$3) may be due to a heterogeneous

Ce distribution within the CAI. The second Allende inclusion with a Ce depletion (HAL) has counterparts in the Dhajala and Murchison chondrites [36,39]. They all have large Ce depletions with normalized La/Ce ratios of ~540 in HAL, ~1770 in DH-H1, ~ 1650 in MU7-971, and ~33 in MU7-404. The two Murchison CAIs also show isotopic characteristics that relate them to HAL and Dhajala DH-H1 [40]. Small Ce depletions have also been reported in CAIs from Cold Bokkeveld, Efremovka, Leoville, Mokoia, Ornans, and Vigarano [31].

analyses of CAIs in other meteorites

Table 2 lists ~ 280 CAIs from 19 chondrites. The REE patterns observed are generally similar to those seen in Allende and Murchison. In particular, CAIs from CV chondrites resemble those from Allende, whereas CAIs from CM chondrites resemble those from Murchison. The small number of CAI analyses for most chondrites precludes detailed comparisons. However it is interesting to note the complete absence of ultrarefractory CAIs in Allende and the more common occurrence of ultrarefractory CAIs in Murchison and in Ornans. Allende is richer in Group II inclusions [8], but CAIs contribute $\leq$ 30% of all the REE in Allende [41], so the Group II signature is diluted by the REE present in chondrules and matrix, and by other CAIs with unfractionated REE patterns.

REE ANALYSES IN OLDHAMITE

Oldhamite (CaS) and the other refractory minerals (e.g.,osbornite TiN, niningerite MgS, alabandite MnS) found in enstatite chondrites are analogs to the minerals found in CAIs [42-44]. Larimer [43-44] showed that CaS, MgS, TiN, etc. are unstable at oxygen fugacities appropriate for solar composition gas ($H_2O/H_2 \sim 5 \times 10^{-4}$) and are only stable under more reducing conditions ($H_2O/H_2 \sim 0.8 \times 10^{-4}$). Conversely, neither perovskite nor hibonite are stable under the reducing conditions where CaS forms.

As summarized by Larimer and Ganapathy [45], selective dissolution experiments and analyses of meteorite fragments with different abundances of oldhamite and other minerals suggested that CaS was the host phase for REE in enstatite chondrites. However REE analyses of pure CaS, TiN, MgS, etc. in enstatite chondrites are difficult because the refractory minerals in enstatite chondrites are generally fine-grained and widely dispersed unlike the easily recognized CAIs in carbonaceous chondrites, and CaS is hygroscopic and difficult to handle. As a result less work has been done on CaS than on minerals in CAIs.

The first REE analysis of oldhamite was done by Larimer and Ganapathy [45] who used neutron activation to determine La, Ce, Sm, Eu, Tb, and Yb in oldhamite grains from the Abee, Indarch, and Yilmia chondrites. Their results showed that the LREE are more enriched than the HREE in Indarch and Yilmia, but only Eu could be measured in a composite enstatite + CaS grain from Abee. Larimer and Ganapathy [46] also analyzed TiN and sinoite Si_2N_2O from Yilmia but found low levels of the REE.

More recently, ion microprobe analyses of the REE [47-48] have been done on oldhamite from Indarch, Jajh deh Kot Lalu, and Qingzhen and on niningerite from Indarch and ALHA77156. This work confirmed that CaS is the major host for the REE. Fairly smooth REE patterns were found in CaS from Indarch and an unfractionated REE pattern with an Eu depletion was reported for CaS in Jajh deh Kot Lalu. Essentially unfractionated patterns, except for Eu and Yb excesses were also found in several oldhamites from Qingzhen, the most primitive enstatite chondrite. The ion microprobe analyses also showed

that some of the Qingzhen oldhamites were isotopically anomalous and had deficits in ^{48}Ca. These deficits are signatures of incomplete isotopic homogenization in the solar nebula and imply that the CaS is a nebular condensate. However, the limited data on REE in CaS do not show any highly fractionated REE patterns analogous to the Group II patterns in CAIs.

INTERPRETATION OF REE ABUNDANCES IN CAIs

condensation and vaporization models

The REE are enriched in CAIs because they form refractory compounds which are stable at high temperatures in solar composition gas. Mineralogical studies of a large number of CAIs have occassionally found REE-rich trace phases in CAIs [13], but the REE are more commonly found dissolved in perovskite, hibonite, and for Eu in melilite. Furthermore, the total REE inventory in a CAI can be accounted for by the amounts of the REE dissolved in these known host phases. Thus gas-solid partitioning of the REE between the solar nebula gas and a few host phases apparently determined REE abundances in CAIs.

As reviewed by Boynton [34], Group II CAIs are produced by a three step fractional condensation process: (1) the most refractory REE (Lu, Er, Ho, Tb, Tm, Dy, Gd) condense into solid grains that are isolated from further vapor-solid reactions, (2) the LREE, which are less refractory, continue to condense into other solid grains, (3) these grains are later also isolated from further vapor-solid reactions prior to condensation of Eu and Yb, the most volatile REE. Boynton [34] also emphasized that the Group II inclusions must be condensates because they are depleted in both the most refractory and the most volatile REE. These depletions are illustrated in Figure 2 where the mean REE abundances in 25 Group II Allende CAIs are plotted. The most refractory REE (Lu and Er) are depleted to C1 chondritic abundances, the most volatile REE (Eu and Yb) are $\sim$ 5 times their C1 abundances, while the intermediate volatility REE (La, Ce, Pr, Nd, Sm) are $\sim$ 30 times their C1 abundances.

Calculated fits to Group II REE patterns place constraints on the temperatures needed to produce the patterns [35,49]. The computational method used and references to the relevant thermodynamic data are given by Kornacki and Fegley [29]. Assuming ideal solid solution, the REE condensation calculations show that Group II patterns in perovskite indicate temperatures approximately equal to the perovskite condensation temperature [49]. This is 1677 K at 10^{-3} bars, 1529 K at 10^{-5} bars, and 1404 K at 10^{-7} bars [19]. Likewise, Group II patterns in hibonite are found to indicate temperatures close to the hibonite condensation temperature [35]. This is 1730 K at 10^{-3} bars, 1548 K at 10^{-5} bars, and 1401 K at 10^{-7} bars [19]. Thus temperatures at least this high are required to make Group II patterns in the solar nebula.

Condensation models can also be used to explain the general characteristics of the other types of REE patterns observed in CAIs. Thus, the Group V pattern is formed when solid grains remain in contact with the nebular gas down to sufficiently low temperatures for all the REE to have completely condensed, while the Group III pattern is formed when the grains are isolated from the gas at slightly higher temperatures where Eu and Yb are mostly still in the gas. Likewise, the Group I and Group VI patterns can be formed by the addition of Eu and Yb rich material to solid grains containing all the other REE. Alternatively, all of these REE patterns could have been formed by the vaporization of chondritic material. As noted by several investigators, the essentially unfractionated character of the Group I,III,V,

and VI patterns does not require an origin by condensation (e.g.,[29,50]).

evidence for oxidizing conditions

Likewise, the Ce depletions observed in several CAIs place constraints on the oxygen fugacity of the ambient environment because CeO_2 is the dominant Ce gas while either the monatomic vapor or monoxides are the dominant gases for the other REE. As a consequence, Ce condensation proceeds via the reaction $CeO_2(g) = CeO_{1.5}(s) + \frac{1}{4}O_2(g)$ while the REE predominantly present as monoxides (e.g., La, Pr, Nd, Gd, Tb, Dy, Ho, Er, Lu) condense via the reaction $MO(g) + \frac{1}{4}O_2 = MO_{1.5}(s)$ and the REE either predominantly or substantially present as monatomic vapor (e.g., Sm, Eu, Tm, Yb) condense via the reaction $M(g) + \frac{3}{4}O_2 = MO_{1.5}(s)$. Thus, an increase in the oxygen fugacity will favor $CeO_2(g)$, making Ce more volatile, while the other REE will become more refractory [34]. This can occur either during condensation or during vaporization as shown experimentally by Nagasawa and Onuma [51]. However, the degree to which other REE such as Sm, Eu, Tm, and Yb (with a dominant or substantial amount of monatomic vapor) will become more refractory relative to REE such as La, Pr, Nd, etc. (dominantly present as monoxides) will also depend on gas phase equilibria between M(g) and MO(g).

unresolved issues with condensation and vaporization models

As outlined earlier, the Group II CAIs formed by a multistage condensation process because they are depleted in both the most refractory and most volatile REE. Furthermore, the loss of the most refractory REE takes place as soon as either hibonite or perovskite starts to condense in the solar nebula, otherwise the Group II pattern is not produced [35,49]. However, since hibonite and perovskite are also the most refractory Ca and Ti-bearing condensates [19], all the Ca and Ti are in the nebular gas at higher temperatures. Thus, Ca and Ti would be isotopically homogenized on a short time scale by nebular mixing and by molecular diffusion instead of being isotopically anomalous as commonly observed in Group II CAIs where isotopic measurements have been made.

Ion microprobe analyses of Murchison Group II CAIs show that the ^{50}Ti, ^{49}Ti, and ^{47}Ti anomalies are *not* correlated and do not all decrease in unison. It is not clear if the anomalies in ^{42}Ca, ^{43}Ca, and ^{48}Ca behave similarly because the ^{42}Ca and ^{43}Ca anomalies are generally not resolvable from zero within 2σ error. Thus, simple dilution by nebular mixing of isotopically anomalous vapor cannot explain the observed Ti isotopic anomalies in Group II CAIs. Alternatively, as suggested by several authors [37,50,52], the Ca and Ti isotopic anomalies in the Group II CAIs could be a signature of presolar chemical processing. In these models the Group II fractionation could either be due to a fractional condensation process in a stellar atmosphere or could be due to a more complex sequence of stellar condensation and nebular processing. For example, the ultrarefractory REE could have been fractionated from the less refractory REE during condensation in an expanding stellar envelope with the subsequent depletion of the most volatile REE (Eu and Yb) occuring during partial vaporization of this presolar dust in the solar nebula. The attractive feature of this model is that both the Ca and Ti isotopic anomalies are inherited from the presolar dust, which is incompletely vaporized and thermally processed in the solar nebula. This model can be tested experimentally by using techniques such as Nd-Sm, La-Ce, or Lu-Hf dating to determine when the depletion of the ultrarefractory REE took place [53].

Another unresolved issue is exactly how the Ce depletions seen in several CAIs were produced. The small Ce depletion reported for the Allende inclusion C1 may be due to a heterogeneous distribution of Ce within the inclusion and may not actually represent a Ce depletion in the bulk inclusion [38]. Other small Ce depletions may simply be due to the greater volatility of Ce relative to that of the neighboring LREE. However, the larger Ce depletions observed in several hibonite-bearing CAIs almost certainly were caused by oxidizing conditions. The question that remains to be answered for these inclusions is how oxidizing the surrounding vapor was and whether the Ce depletions indicate condensation under oxidizing conditions or vaporization under oxidizing conditions.

The occasional presence of Pr depletions in some hibonite-bearing CAIs from the Murchison and Dhajala chondrites [36,39] is also unexplained. Fegley [54] originally noted that Pr, like Ce, has a stable dioxide gas and thus will behave similarly to Ce under appropriately oxidizing conditions. Pr depletions are less common than Ce depletions, which suggests qualitatively that higher oxygen fugacities are required to deplete Pr. However, further information is needed on Pr depletions in CAIs and on thermodynamic data for PrO_2 gas before a quantitative explanation is possible.

Finally, the REE patterns in oldhamite also need to be modelled. The available theoretical work [55-56] indicates that REE condensation into oldhamite occurs under a restricted range of P,T, and f_{O_2} conditions and thus is potentially an important constraint on the oxidation state of the nebula in the enstatite chondrite formation region. Furthermore, the preferential LREE enrichments observed in oldhamites from the Indarch and Yilmia chondrites [45] are consistent with vapor-solid partitioning of the REE under reducing conditions. However, both more REE analyses of oldhamites and detailed models of REE condensation under reducing conditions are needed to improve our knowledge in this area.

ACKNOWLEDGMENTS

B.F. was supported by the MPI für Chemie, and T.I. was supported by a Queen Elizabeth II fellowship at ANU. We thank H. Palme and B. Spettel for the bulk Murchison analysis in Fig.2 and K. Lodders, H. Palme, and T. Presper for discussions. This is LPI Contribution No. 753.

REFERENCES

[1] I. NODDACK, *Z. Anorg. Allgem. Chem.*, 1935, **225**, p. 337.
[2] R.A. SCHMITT, A.W. MOSEN, C.S. SUFFRENDINI, J.E. LASCH, R.A. SHARP, and D.A. OLEHY, *Nature*, 1960, **186**, p. 863.
[3] E. ANDERS and N. GREVESSE, *Geochim. Cosmochim. Acta*, 1989, **53**, p. 197.
[4] H.E. SUESS and H.C. UREY, *Rev. Mod. Phys.*, 1956, **28**, p.53.
[5] J.T. WASSON and G.W. KALLEMEYN, *Phil. Trans. R. Soc.*, 1988, **325A**, p. 535.
[6] J.W. LARIMER and J.T. WASSON, in "Meteorites and the Early Solar System," p. 394, Univ. of Arizona Press, Tucson, AZ, 1988.
[7] N.M. EVENSEN, P.J. HAMILTON, and R.K. O'NIONS, *Geochim. Cosmochim. Acta*, 1978, **42**, p. 1199.
[8] B. FEGLEY, JR. and A.S. KORNACKI, *Lunar Planet. Sci.*, 1984, **XV**, p. 262.
[9] D.B. CURTIS and R.A. SCHMITT, *Geochim. Cosmochim. Acta*, 1979, **43**, p. 1091.
[10] G. CROZAZ and E. ZINNER, *Earth Planet. Sci. Lett.*, 1985, **73**, p. 41.
[11] A. BISCHOFF AND K. KEIL, *Geochim. Cosmochim. Acta*, 1984, **48**, p. 693.
[12] A. BISCHOFF, K. KEIL, and D. STÖFFLER, *Chem. Erde*, 1985, **44**, p. 97.
[13] G.J. MACPHERSON, D.A. WARK, and J.T. ARMSTRONG, in "Meteorites and the Early Solar System," p. 746, Univ. of Arizona Press, Tucson, AZ, 1988.

[14] R.S. CLARKE, JR., E. JAROSEWICH, B. MASON, J. NELEN, J. GÓMEZ, and J.R. HYDE, *Smithsonian Contrib. Earth Sci.*, 1970, **5**, 53 pp.
[15] U.B. MARVIN, J.A. WOOD, & J.S. DICKEY, *Earth Planet. Sci. Lett*, 1970, **7**, p. 346.
[16] H.C. LORD III, *Icarus*, 1965, **4**, p. 279.
[17] J.A. LARIMER, *Geochim. Cosmochim. Acta*, 1967, **31**, p. 1215.
[18] R.E. COHEN, A.S. KORNACKI, & J.A. WOOD, *Geochim. Cosmochim. Acta*, 1983, **47**, p. 1739.
[19] A.S. KORNACKI and B. FEGLEY, JR., *Proc. 14th Lunar Planet. Sci. Conf., J. Geophys. Res. Suppl.*, 1984, p. B588.
[20] A.S. KORNACKI and J.A. WOOD, *Geochim. Cosmochim. Acta*, 1985, **49**, p. 1219.
[21] L. GROSSMAN, *Geochim. Cosmochim. Acta*, 1972, **36**, p. 597.
[22] P.W. GAST, N.J. HUBBARD, and H. WIESMANN, *Proc. Apollo 11 Lunar Sci. Conf.*, 1970, p. 1143.
[23] L. GROSSMAN, *Geochim. Cosmochim. Acta*, 1973, **37**, p. 1119.
[24] H. WÄNKE, H. BADDENHAUSEN, H. PALME, and B. SPETTEL, *Earth Planet. Sci. Lett.*, 1974, **23**, 1.
[25] T. TANAKA and A. MASUDA, *Icarus*, 1973, **19**, p. 523.
[26] P.M. MARTIN and B. MASON, *Nature*, 1974, **249**, p. 333.
[27] B. MASON and P.M. MARTIN, *Smithsonian Contrib. Earth Sci.*, 1977, **19**, p. 84.
[28] B. MASON and S.R. TAYLOR, *Smithsonian Contrib. Earth Sci.*, 1982, **25**, 30 pp.
[29] A.S. KORNACKI and B. FEGLEY, JR., *Earth Planet. Sci. Lett.*, 1986, **79**, p. 217.
[30] E. JAROSEWICH, R.S. CLARKE, JR., and J.N. BARROWS, *Smithsonian Contrib. Earth Sci.*, 1987, **27**, 49 pp.
[31] B. FEGLEY, JR. and T.R. IRELAND, *Lunar Planet. Sci.*, 1991, **XXII**, in prep.
[32] A.S. KORNACKI and J.A. WOOD, *Proc. 14th Lunar Planet. Sci. Conf., J. Geophys. Res. Suppl.*, 1984, p. B573.
[33] A.S. KORNACKI and J.A. WOOD, *Earth Planet. Sci. Lett.*, 1985, **72**, p. 74.
[34] W.V. BOYNTON, in "Rare Earth Element Geochemistry," p. 63, Elsevier, Amsterdam, 1983.
[35] V. EKAMBARAM, I. KAWABE, T. TANAKA, A.M. DAVIS, and L. GROSSMAN, *Geochim. Cosmochim. Acta*, 1984, **48**, p. 2089.
[36] T.R. IRELAND, A.J. FAHEY, & E.K. ZINNER, *Geochim. Cosmochim. Acta*, 1988, **52**, p. 2841.
[37] T.R. IRELAND, *Geochim. Cosmochim. Acta*, 1990, in press.
[38] I. HUTCHEON, H. PALME, A. KENNEDY & B. SPETTEL, *Meteoritics*, 1989, **24**, p.279.
[39] R.W. HINTON, A.M. DAVIS, D.E. SCATENA-WACHEL, L. GROSSMAN, and R.J. DRAUS, *Geochim. Cosmochim. Acta*, 1988, **52**, p. 2573.
[40] T.R. IRELAND, A.J. FAHEY, and E.K. ZINNER, *Lunar Planet. Sci.*, 1989, **XX**, p. 442.
[41] T.R. IRELAND, H. PALME, and B. SPETTEL, *Lunar Planet. Sci.*, 1990, **XXI**, p. 546.
[42] D.W.G. SEARS, *Icarus*, 1980, **43**, p. 184.
[43] J.W. LARIMER, *Geochim. Cosmochim. Acta*, 1975, **39**, p. 389.
[44] J.W. LARIMER and M. BARTHOLOMAY, *Geochim. Cosmochim. Acta*, 1979, **43**, p. 1455.
[45] J.W. LARIMER and R. GANAPATHY, *Earth Planet. Sci. Lett.*, 1987, **84**, p. 123.
[46] J.W. LARIMER and R. GANAPATHY, *Meteoritics*, 1983, **18**, p. 334.
[47] L.L. LUNDBERG and G. CROZAZ, *Meteoritics*, 1988, **23**, p. 285.
[48] L.L. LUNDBERG, G. CROZAZ, E. ZINNER, & A. EL GORESY, *Meteoritics*, 1989, **24**, p. 296.
[49] A.M. DAVIS and L. GROSSMAN, *Geochim. Cosmochim. Acta*, 1979, **43**, p. 1611.
[50] J.A. WOOD, *Earth Planet. Sci. Lett.*, 1981, **56**, p. 32.
[51] H. NAGASAWA and N. ONUMA, *Lunar Science*, 1979, **X**, p. 884.
[52] A.S. KORNACKI and B. FEGLEY, JR., *Lunar Planet. Sci.*, 1985, **XVI**, p. 457.
[53] B. FEGLEY, JR. and A.S. KORNACKI, *Earth Planet. Sci. Lett.*, 1984, **68**, p. 181.
[54] B. FEGLEY, JR., *Lunar Planet. Sci.*, 1986, **XVII**, p. 220.
[55] B. FEGLEY, JR. *Meteoritics*, 1982, **17**, p.210.
[56] J.W. LARIMER, H.A. BARTHOLOMAY, and B. FEGLEY, JR., *Meteoritics*, 1984, **19**, p.258.

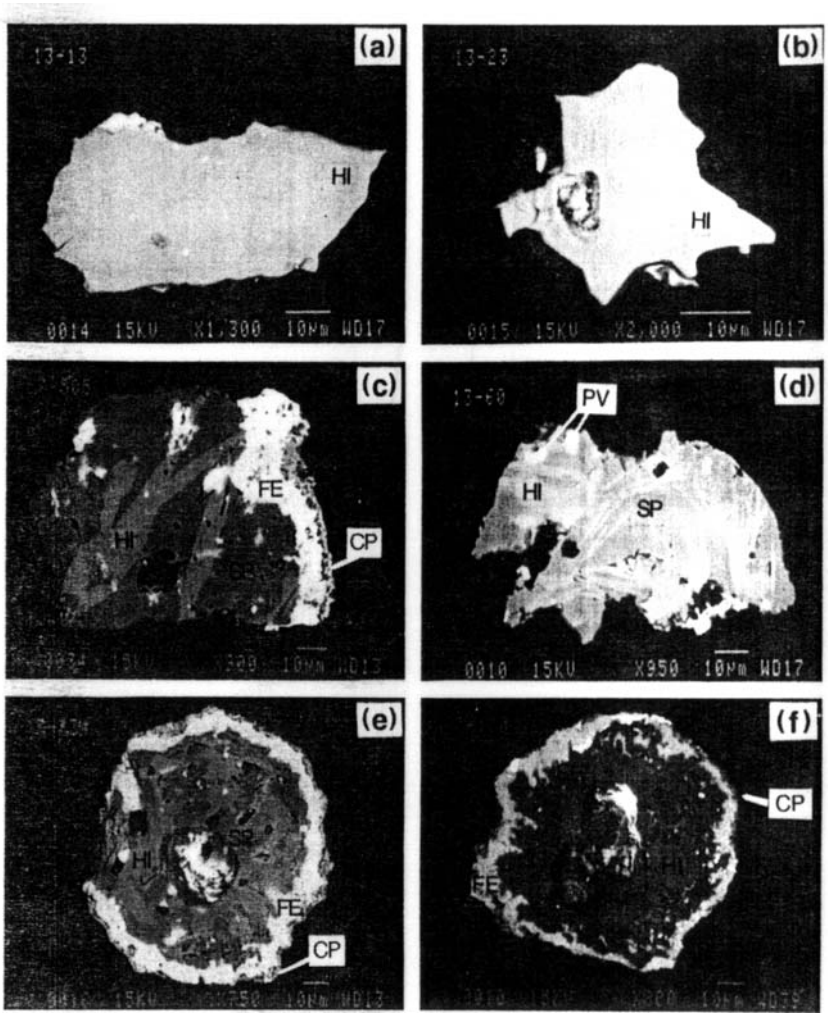

Figure 1. Back-scattered electron images of CAIs from the Murchison CM2 chondrite. A variety of inclusions has been found which have characteristic morphological, chemical, and isotopic features. Inclusions 13-13 (a) and 13-23 (b) consist predominantly of hibonite and have large Ca and Ti isotopic anomalies; 13-13 has a Group III pattern with evidence for igneous fractionation while 13-23 has a Group II pattern with low overall abundances of the REE. The other four inclusions (c-f) consist of hibonite, spinel, minor perovskite. Rims composed of lower temperature minerals are also apparent. These inclusions generally have small Ca and Ti isotopic anomalies and Group II REE patterns. However, 7-734 and 7-170 (e,f), while morphologically and chemically very similar, have markedly different isotopic systematics (as discussed in text). Ion probe pits are apparent in (e) and (f) with residual gold coating. [Scale bar for all figures is 10 μm; Minerals: HI = hibonite, SP = spinel, PV = perovskite, FE = iron phyllosilicate, CP = clinopyroxene.]

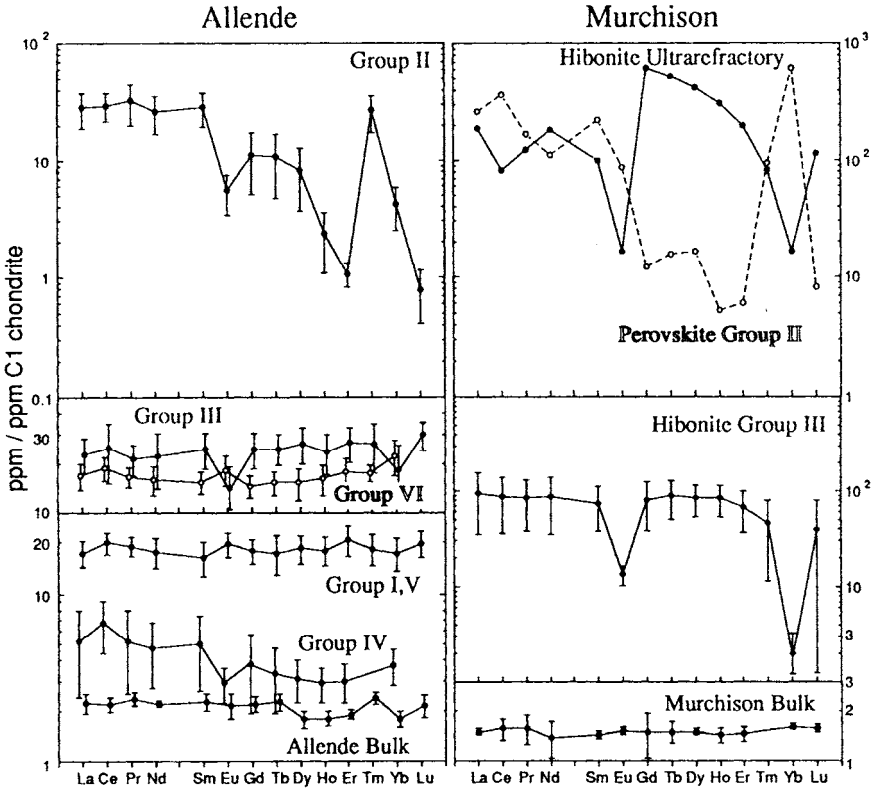

Figure 2. Rare earth element patterns in CAIs from the Allende and Murchison carbonaceous chondrites; see text for complete descriptions. Bulk measurements of Allende and Murchison are also shown.

Table 2. REE classification of 283 CAIs.

	I,V	II	III	IV*	VI	Ultra	UC	HAL	Total
Allende	54	35	12	3	6			1	111
Arch	1								1
Cold Bok.			2						2
Dhajala								1	1
Efremovka	2	1					1		4
Essebi						1			1
Felix			1						1
Grosnaja	2								2
Kaba		1	7	12			2		22
Lancé	1	1							2
Leoville	4	3							7
Mighei			1						1
Mokoia		5							5
Murchison	5	33	35			6		2	81
Murray	1	5	2			1			9
Omans		1				3			4
Semarkona		1							1
Vigarano	8	3	2				1		14
ALH85085	2	8	1		1		2		14
Total	80	97	63	15	7	11	6	4	283
%	28.3	34.3	22.3	5.3	2.5	3.9	2.1	1.4	